Geophysical Research Letters

RESEARCH LETTER
10.1029/2019GL083978

Special Section:
Community Earth System Model version 2 (CESM2) Special Collection

High Climate Sensitivity in the Community Earth System Model Version 2 (CESM2)

A. Gettelman[1], C. Hannay[1], J. T. Bacmeister[1], R. B. Neale[1], A. G. Pendergrass[1], G. Danabasoglu[1], J.-F. Lamarque[1], J. T. Fasullo[1], D. A. Bailey[1], D. M. Lawrence[1], and M. J. Mills[1]

[1]National Center for Atmospheric Research, Boulder, CO, USA

Abstract The Community Earth System Model Version 2 (CESM2) has an equilibrium climate sensitivity (ECS) of 5.3 K. ECS is an emergent property of both climate feedbacks and aerosol forcing. The increase in ECS over the previous version (CESM1) is the result of cloud feedbacks. Interim versions of CESM2 had a land model that damped ECS. Part of the ECS change results from evolving the model configuration to reproduce the long-term trend of global and regional surface temperature over the twentieth century in response to climate forcings. Changes made to reduce sensitivity to aerosols also impacted cloud feedbacks, which significantly influence ECS. CESM2 simulations compare very well to observations of present climate. It is critical to understand whether the high ECS, outside the best estimate range of 1.5–4.5 K, is plausible.

Key Points:
- The Community Earth System Model Version 2 (CESM2) has an Equilibrium Climate Sensitivity (ECS) of 5.3 K
- ECS change is mostly due to atmospheric cloud feedbacks, with land surface impacts in intermediate versions
- Processes that impact ECS through cloud feedbacks also impact aerosol forcing of climate

Supporting Information:
- Supporting Information S1

Correspondence to:
A. Gettelman,
andrew@ucar.edu

Citation:
Gettelman, A., Hannay, C., Bacmeister, J. T., Neale, R. B., Pendergrass, A. G., Danabasoglu, G., et al. (2019). High climate sensitivity in the Community Earth System Model Version 2 (CESM2). *Geophysical Research Letters*, *46*, 8329–8337. https://doi.org/10.1029/2019GL083978

Received 20 MAR 2019
Accepted 9 JUL 2019
Accepted article online 16 JUL 2019
Published online 22 JUL 2019

1. Introduction

The evolution of future climate is dictated by how climate will be forced and how it will respond to the forcing. The forcing is often amplified or damped by internal responses to the forcing or "feedbacks" (Cess et al., 1989, 1990). The sensitivity of the climate system to a forcing is an important metric of the impact of a given forcing on climate. The equilibrium climate sensitivity, or ECS, measures the sensitivity of a system equilibrated to a forcing, often the forcing associated with a doubling of carbon dioxide (CO_2) from preindustrial (PI) levels. ECS is defined as

$$ECS = \Delta T_s = -\lambda F, \tag{1}$$

where ΔT_s is the equilibrium change in surface temperature, F is the forcing, and λ is the climate sensitivity parameter (Cess et al., 1990). The climate sensitivity parameter λ is the inverse of the climate feedback parameter, $\gamma = 1/\lambda$, which has units of Watts per square meter per degree ($W{\cdot}m^{-2}{\cdot}K^{-1}$; Gettelman, Kay, & Shell, 2012).

The Transient Climate Sensitivity measures the response of the climate system before it has reached equilibrium, typically after a certain time (often a CO_2 doubling with ramped forcing). While Transient Climate Sensitivity may be a better metric for comparison to observations and estimating near term climate response (Knutti et al., 2017), ECS has a long history as a convenient metric of future climate change. The range of best estimate ECS values of 1.5 to 4.5 ° C has changed little between Charney (1979) and Stocker et al. (2013), though the simulated ECS range from models is broader than this (e.g., Tian, 2015).

This work documents the ECS of the most recent version of the Community Earth System Model Version 2 (CESM2) as 5.3 K. To understand the ECS, we quantify the forcing and feedbacks in CESM2. This paper presents initial ECS results with partial explanations for ECS changes from CESM1, and an exhortation to the community to help fully understand the climate sensitivity of CESM2 and compare it to other models.

Section 2 describes the model, analysis methodology, and simulations. Section 3 analyzes the climate sensitivity (section 3.1), feedbacks (section 3.2), and forcing (section 3.3) in CESM2. Section 4 discusses the CESM2 model development process, and preliminary conclusions from this work are in section 5.

2. Methodology

Our goal is to present quantitative estimates of climate sensitivity and the contributions of feedback and forcing. First we look at ECS with coupled forcing and response experiments, then we analyze feedbacks

with specified surface temperature change, and finally, we impose an atmospheric aerosol forcing with fixed temperatures to look at radiative and physical responses.

2.1. Climate Sensitivity

Climate sensitivity is defined as the global average surface temperature change in response to a forcing. The forcing is defined as the (mostly clear-sky longwave [LW]) response to a doubling of the CO_2 concentration from 284.7 to 569.4 ppm, approximately 3.8 Wm^{-2} (Collins et al., 2006). ECS is estimated as the temperature change in response to a forcing when the system has reached equilibrium (equation (1)). We will focus on the ECS response using slab ocean model (SOM) simulations (sometimes called a mixed layer model), where the deep ocean heat flux is prescribed and normalized to have a global annual mean of zero. Danabasoglu and Gent (2009) have shown that SOM ECS results are representative of fully coupled simulations.

2.2. Feedback

Climate feedbacks (γ) are a significant component of the climate change signal (e.g., Bony et al., 2006; Charney, 1979; Cess et al., 1990). The sum of feedbacks are negative, dominated by the increased LW emission as blackbody emission temperature rises. Water vapor feedbacks are positive (Cess, 2005; Held & Soden, 2000) and coupled to a negative lapse-rate feedback (a warmer atmosphere with more water vapor has a higher emission level; Folkins, 2002). Surface albedo feedbacks (Colman, 2013) result from changing surface albedo (mostly from ice and snow) in a warmer (or cooler) climate. Clouds are the largest uncertainty in total feedbacks and ECS (Stocker et al., 2013). Cloud feedbacks (CFs) involve a complex mix of processes (Gettelman & Sherwood, 2016; Stephens, 2005).

Feedbacks are estimated with radiative kernels following Soden et al. (2008). Kernels for atmosphere and surface temperature, water vapor, surface albedo, and CO_2 are used to estimate the radiative response. CFs are defined as the kernel-adjusted CF, where the effects of other feedbacks are removed from the change in cloud radiative effect (CRE = all sky radiation minus clear-sky radiation). The methodology was applied to CCSM3 by Shell et al. (2008) and to CESM1 by Gettelman, Kay, and Shell (2012) and Gettelman et al. (2013) and has been used by numerous other authors (e.g., Webb et al., 2012; Vial et al., 2017). Kernels are calculated with CAM3 (Shell et al., 2008). Analysis with CAM5 kernels yields qualitatively similar results (Pendergrass et al., 2018).

2.3. Forcing

Climate forcing comes from many sources beyond greenhouse gases, including natural sources (aerosols, volcanoes, and solar variability) and anthropogenic aerosols. The forcing uncertainty associated with anthropogenic long- and short-lived greenhouse gases is small compared with the uncertainty due to anthropogenic aerosols (Boucher et al., 2013; Stocker et al., 2013). Aerosols alter cloud condensation nuclei, leading to higher cloud drop number concentrations and smaller particle sizes. The resulting shortwave (SW) "brightening" of liquid clouds results in a cooling effect (Twomey, 1977). The change in drop number may also alter clouds in complex ways, either increasing cloud thickness and or lifetime (Albrecht, 1989) or even decreasing it due to buffering processes (Ackerman et al., 2004; Stevens & Feingold, 2009). The effect of anthropogenic sulfur emissions on low clouds is the largest uncertainty for radiative forcing of climate (Boucher et al., 2013).

Changes to atmospheric composition (either aerosols or greenhouse gases) also induce other changes to the climate system, which are not purely a function of surface temperature. These are known as rapid adjustments (Hansen et al., 2005) and involve changes to clouds or the surface. Consequently, radiative forcing is often characterized as the combination of the forcing and fast adjustments, or the Effective Radiative Forcing (ERF; Sherwood et al., 2015). This work will include fast adjustments, and further references to "forcing" imply ERF.

We can estimate the total aerosol effect (direct + indirect) as the total change in top of atmosphere radiative flux between a pair of simulations with different aerosol loading. Aerosol-cloud interactions (ACIs) are quantified as the change in CRE. Estimates are calculated separately for LW and SW bands.

2.4. Model Description

CESM2 is a comprehensive Earth system model with coupled atmosphere, land, ocean, sea ice, and ice sheets. CESM2 is participating in the Coupled Model Intercomparison Project Phase 6 (CMIP6; Eyring et al., 2016). The atmospheric component of CESM2 is CAM6 (see the supporting information). We focus on

Table 1
Table of ECS from CESM1 and CESM2 SOM simulations

Sim. Nam	Atmos.	Ocean	Land/ice	ECS
CESM1	CESM1.2	CESM1.2	CESM1.2	4.0
CESM2d125	CESM2d125	CESM2d125	CESM2d125	4.4
CESM2-LndAtm	CESM2d125	CESM2	CESM2d125	4.3
CESM2-Atm	CESM2d125	CESM2	CESM2	4.9
CESM2-AtmOcn	CESM2d125	CESM2d125	CESM2	4.9
CESM2	CESM2	CESM2	CESM2	5.3

Note. ECS = equilibrium climate sensitivity; SOM = slab ocean model; CESM = Community Earth System Model. Two CESM2 SOM simulations have the same sensitivity (5.3 K).

the atmosphere component because it governs gas and aerosol forcing and is responsible for many critical climate feedbacks, in particular clouds.

CESM2 produces a very good representation of the current climate (see the supporting information). CESM1 was among the models that compared best to observations for CMIP5 (Knutti et al., 2013), and CESM2 improves upon this, as illustrated in Figure S1 and Table S1. CESM2 also reproduces the surface temperature time series over the twentieth century (Figure S2). In numerous ways, CESM2 is the best and most comprehensive Earth system model in the CCSM and CESM series. CESM1 (Hurrell et al., 2013) refers to CESM1.2 as described by Kay et al. (2014). Specific model simulations identified here for forcing and feedback experiments are described in detail in the supporting information.

2.5. Simulations

To assess ECS, feedbacks, and aerosol forcing, we use three sets of CESM experiments. These are detailed in the supporting information, with the key features identified here. Set 1 is SOM simulations with the atmosphere and land coupled to a simplified ocean mixed layer above the thermocline, with imposed ocean heat flux. Simulations are performed with present day (PD) and instantaneously doubled CO_2. SOM simulations are performed with CESM2, CESM1, and an interim version "CESM2d125." Perturbation experiments explore the changes to the atmosphere, ocean, and land surface between CESM2d125 and CESM2.

The second set of simulations isolates atmospheric feedback processes responsible for ECS. Set 2 uses fixed sea surface temperature (SST) forcing experiments to impose an idealized temperature change between simulations with fixed PD SST and simulations with a uniform 4-K increase in SST, following Cess et al. (1990) and Gettelman, Kay, and Shell (2012). We remove one parameterization at a time from CAM6, to elucidate changes in feedbacks.

The third set of simulations analyzes the physical and radiative response to changing aerosols and aerosol-cloud processes with fixed SST experiments using different aerosol emissions. Forcing is defined as the difference between a pair of simulations with Year 2000 (PD) aerosol emissions and 1850 (PI) aerosol emissions. The anthropogenic direct forcing is defined as the difference in clear-sky ERF. ACI or ERF due to ACI (ERF_{ACI} following Boucher et al., 2013) is defined as CRE_{PD}-CRE_{PI}.

3. Results

3.1. Climate Sensitivity

Table 1 documents ECS in SOM simulations. The "-" in simulation names indicates components reverted to CESM2d125. CESM2 has an ECS of 5.3 ± 0.1 K. Uncertainty in SOM-estimated ECS is ±0.1 K quantified as the 2 standard deviation (2σ) range of the difference of 20-year means of global average temperature. The CESM2d125 configuration, with all the same atmosphere parameterizations as CESM2, has a sensitivity of 4.4 K, larger than CESM1 (4.0 K). This +0.4 K is mostly due to the CAM6 physical parameterizations in the atmosphere (see section 3.2) offset by changes in the land model. Introducing the CESM2 land component between CESM2-LndAtm and CESM2-Atm increases ECS by 0.6 K. The CESM2d125 land model (CLM5d125), a preliminary version of CLM5, exhibited unrealistic and strongly high-biased Leaf Area Index, primary productivity, and evaporation. These biases were alleviated in the final CESM2-CLM5 version. Fixed SST Feedback experiments using CLM4, CLMd125, and CLM5 with the same CAM6 atmosphere indicate

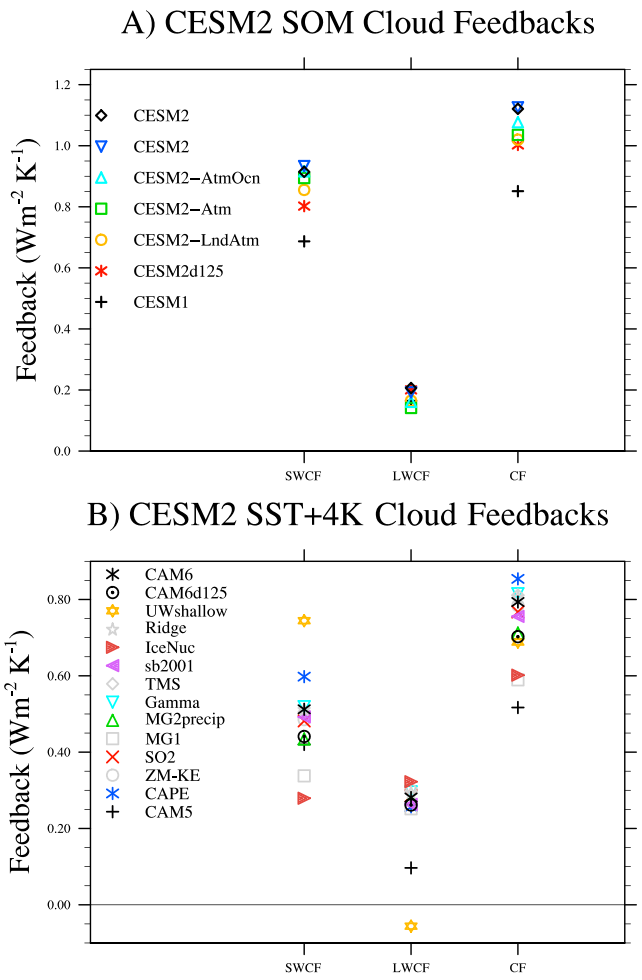

Figure 1. Global average CFs from (a) slab ocean model (SOM) and (b) SST+4 K sensitivity simulations. Perturbations as described in the text. CESM = Community Earth System Model Version 2; SST = sea surface temperature; CF = cloud feedback; SWCF = shortwave cloud feedback; LWCF = longwave cloud feedback.

that CLM5d125 responds more strongly to climate and CO_2 changes than CLM4 or CLM5, with strong increases in evaporation (latent heat flux) in CLM5d125 damping land surface temperature response. Thus, switching from CLM5d125 to CLM5 between CESM2-LndAtm and CESM2-Atm appears to increase ECS, but it is reducing the damping effect of the land from CESM1 (CLM4) to CESM2d125 (CLM5d125).

The ocean and sea ice have little impact on ECS in these experiments. Using a different ocean heat flux (Q_{flux}) to constrain the SOM has virtually no impact. CESM2-LndAtm versus CESMd125 is the effect of the ocean heat flux, and CESM2-Atm and CESM2-AtmOcn have the same ECS with different ocean heat flux. Sea ice changes have virtually no impact on ECS in the SOM. Finally, introducing the CESM2 atmosphere from CESM2-Atm to CESM2 further increases ECS by +0.4 K.

3.2. Feedbacks

A feedback analysis confirms that differences between CESM1 and CESM2 are mostly due to the atmosphere. Radiative kernel calculations are applied to SOM and SST+4-K experiments to isolate atmospheric feedbacks. CFs dominate the differences among simulations, and there are no systematic differences in the other atmospheric feedbacks (Table S3) including vertically uniform temperature, water vapor, lapse rate, or surface albedo feedbacks. Figure 1a illustrates CFs in SOM simulations. SW CF increases consistently from CESM1, through the intermediate perturbations, to CESM2 (two simulations), and this dominates the variation in total CF. SW CF is smaller in CESM2d125 than in CESM2 (Figure 1a and Table S3), resulting in a total CF ~0.1 $W{\cdot}m^{-2}{\cdot}K^{-1}$ lower, which yields ~0.5–1 K of ECS increase. CESM1 CFs are another ~0.1 $W{\cdot}m^{-2}{\cdot}K^{-1}$ lower than CESMd125. The ocean has little effect on total CF with the LW and SW canceling, seen in the difference between CESM2d125 (Figure 1a, red) and CESM2-LndAtm (Figure 1a, yellow). The land changes from CESM2-LndAtm (Figure 1a, yellow) to CESM2-Atm (Figure 1a, green) have only a small impact on CF. Land impacts on ECS between CESM2d125 and CESM2 are not through CFs (section 3.1). The Atmospheric changes (from CESM2-Atm, green, to CESM2) have the largest impact on CFs between CESMd125 and CESM2 (Figure 1a and Table S3).

To elucidate the change in CF strength between the different atmosphere configurations, we evaluate feedbacks in CAM5 and CAM6, and we remove one parameterization at a time in CAM6. Simulations are described in detail in the supporting information (Table S2)—They also overlap the forcing experiments. Figure 1b and Table S3 indicate that CAM5 (black cross) has smaller CF than CAM6 (black asterisk), and CAM6d125 (black circle), the atmosphere for CESM2d125. CF differences between CAM6d125 and CAM6 lie mainly in the SH subtropics (−30 to 0° S) and storm track (−50 to −35° S) regions (Figure 2). Subtropical effects are consistent with large sensitivities of these cloud regimes seen in CAM5 (Gettelman, Liu, et al., 2012) and in many other models (Zelinka et al., 2016).

CF differences between CAM5 and CAM6d125 are larger (+0.18 $W{\cdot}m^{-2}{\cdot}K^{-1}$) than CAM6d125 and CAM6 (+0.09 $W{\cdot}m^{-2}{\cdot}K^{-1}$; Table S3). Based on the feedback parameter $\gamma = -F/\Delta T_s$ (equation (1)) for a doubling of CO_2 with F ~3.8 W/m^2, then for ΔT =5.3 K, $\gamma = -0.72$ $W{\cdot}m^{-2}{\cdot}K^{-1}$ for CAM6. Reducing CF by 0.09 $W{\cdot}m^{-2}{\cdot}K^{-1}$ yields $\Delta T = -F/\gamma = -3.8/0.81 = 4.7$ K (a 0.6-K reduction in sensitivity). Reducing CF from CAM6d125 to CAM5 (another 0.18 $W{\cdot}m^{-2}{\cdot}K^{-1}$) yields $\Delta T = 3.8$ K. This 0.9-K reduction is larger than the 0.4-K SOM ECS change between CESM1 and CESM2d125; thus, other components may have damped ECS changes from CF between CESM1 and CESM2d125.

Figure 2 and Table S3 indicate that the main differences between CAM5 and CAM6d125 come from four changes. (1) The change of stratiform microphysics (MG1; Figure 1b, gray square). (2) The change from the Park and Bretherton (2009) shallow convection scheme in CAM5 to the Cloud Layers Unified by Bi-Normals

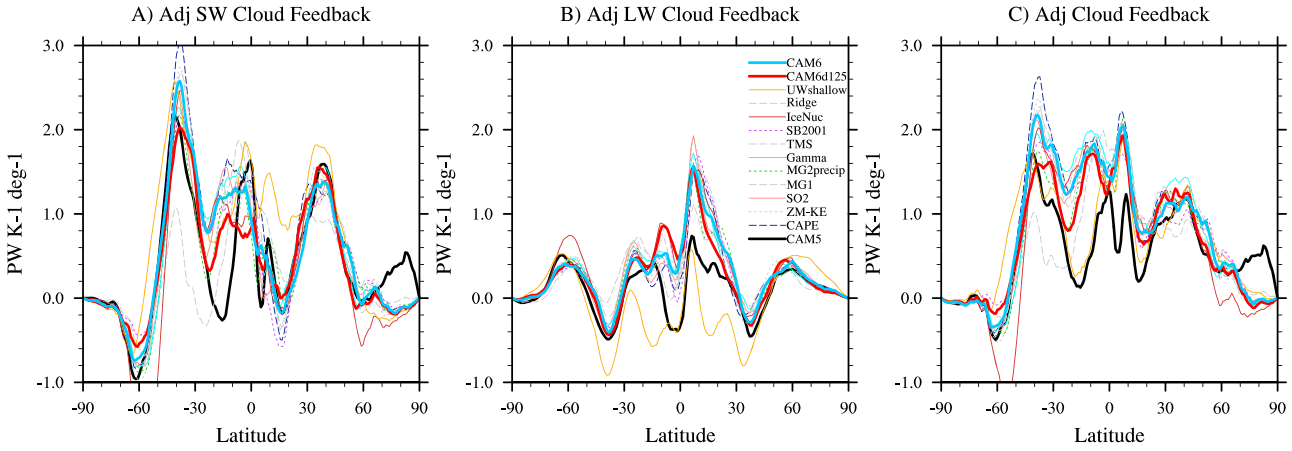

Figure 2. Zonal-mean area-weighted (a) shortwave (SW), (b) longwave (LW), and (c) net kernel-adjusted cloud feedback from SST+4 K sensitivity experiments. Thicker lines represent CAM6 (red), CAM6d125 (black), and CAM5 (blue).

(CLUBB; Bogenschutz et al., 2013) unified moist turbulence scheme in CAM6 (UWshallow). The UWshallow experiment (Figure 1b orange star) has feedbacks more similar to CAM5 in the subtropics (Figure 2c orange). (3) Reverting the CAM6 mixed phase ice nucleation scheme of Hoose et al. (2010) to the Meyers et al. (1992) empirical scheme (IceNuc; Figure 1b, Brown triangle). With Meyers et al. (1992) the IceNuc, CAM5, and MG1 experiments have almost no supercooled liquid water in high-latitude clouds, and a large negative cloud phase feedback when ice turns to liquid. Removal of this negative cloud phase feedback increases net CF in CAM6. CAM5, IceNuc, and MG1 experiments have the lowest total CF in Figure 1b and also contain significant cloud biases in the south. Ocean that have been reduced with MG2 and new ice nucleation (Gettelman et al., 2015), implying CAM6 feedback, is more consistent with current climate. (4) The increase in tropical and subtropical Northern Hemisphere LW cloud feedbacks (LWCF) between CAM5 and CAM6d125 (Figures 1b and 2b) results from increases in LWCF in the tropical Western and Eastern Pacific and Indian Ocean, due to changes in convective parameters between CAM5 and CAM6d125. LWCF changes from CAM5 to CAM6d125 may have affected ECS between CESM1 and CESM2d125.

Other changes affect CF between CAM6d125 and CAM6. The MG2precip experiment reverts an error in the MG2 rain evaporation (see the supporting information), lowering feedbacks (Figure 1b, green triangle). Thus, rain evaporation changes increased CFs in CAM6. In midlatitudes in both hemispheres, the SB2001 autoconversion scheme in CAM6d125 has lower CFs than the modified KK2000 scheme used in CAM6 (Figure 1b, purple triangle). Reverting changes to decrease SO2 lifetime in CAM6 (section 3.3) also lower CFs (Figure 1b, red "X"), indicating higher CF in CAM6. Increasing the extent and optical thickness of low clouds by decreasing vertical velocity PDF width in CLUBB in CAM6 (Gamma; Figure 1b, cyan triangle) tends to increase CFs (larger low cloud decks are more sensitive). Reverting the CAPE convection changes increases tropical CFs (Figure 1b, blue asterix), indicating that these changes between CAM6d125 and CAM6 have a negative (damping) effect on CF.

In summary, different parameterization changes made in the development process from CAM5 to CAM6d125 and CAM6d125 to CAM6 can span the range of CFs between CESM2d125 and CESM2 and contribute to changes in ECS. Note that not all the changes are linear, showing the limits of the one-at-a-time, SST+4 K feedback analysis approach. But the analysis enables attribution of ECS sensitivity to individual processes.

3.3. Aerosol-Cloud Interactions

Several changes were made between CESM1 and CESM2 to the representation of the aerosols and the stratiform cloud microphysics (Gettelman & Morrison, 2015; Gettelman et al., 2015). First, a new representation of the autoconversion (Seifert & Beheng, 2001) was used in CESM2d125, as described in Gettelman (2015) (C6-SB). Then adjustments were made to the original autoconversion scheme (Khairoutdinov & Kogan, 2000) to reduce the sensitivity (C6-KKorig). Importantly, CESM2 uses CMIP6 emissions (Hoesly et al., 2018). We also explored the impact of using CMIP5 emissions (Lamarque et al., 2010). Changes to the emissions

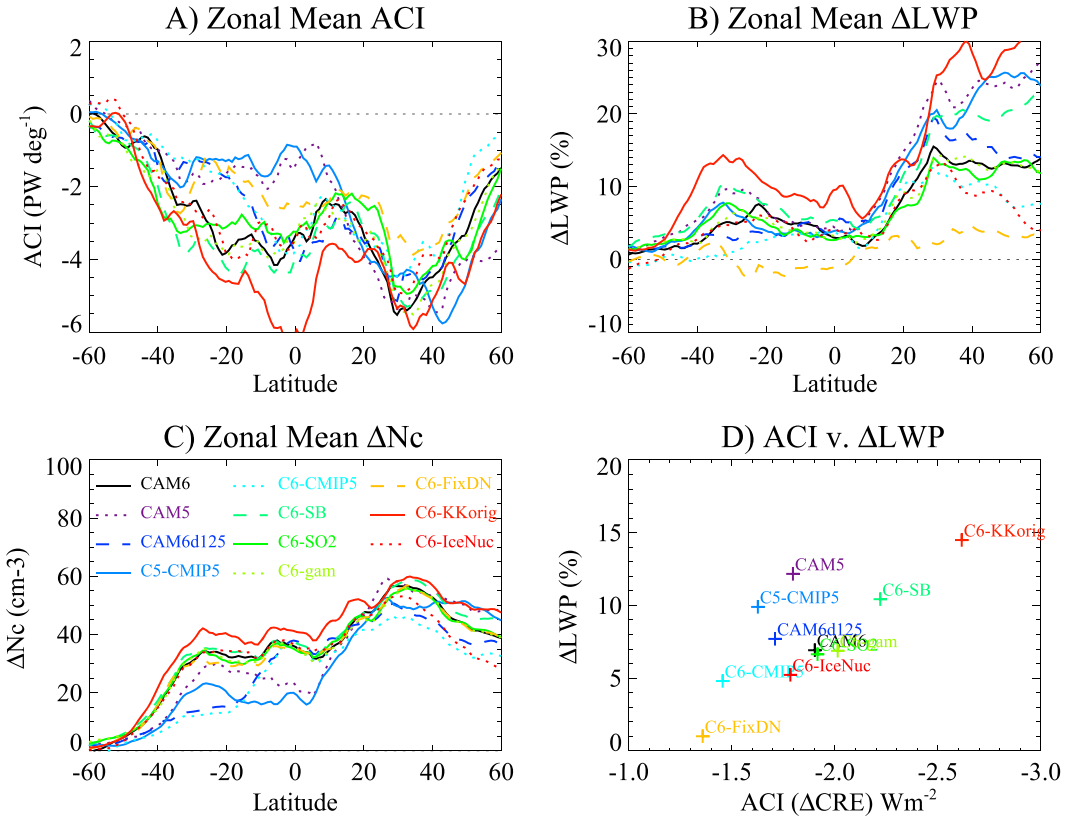

Figure 3. Zonal-mean (a) aerosol-cloud interactions (ACI) (CRE_{PD}-CRE_{PI}), (b) percent change in liquid water path (LWP), (c) change in cloud drop number concentration (Nc), and (d) global-mean ACI versus change in LWP. Different simulations perturb ACI as described in the text.

description, including emissions altitudes and scavenging that affects aerosol lifetime, were also applied to better match aerosol observations, especially of SO2 (C6-SO2).

Figure 3 illustrates results of the sensitivity tests. The change in net CRE (ACI) in CAM6 is −1.9 W/m^2. The total aerosol ERF is −1.67 W/m^2 (Table S4). Using CMIP5 emissions (Lamarque et al., 2010) reduces ACI magnitude to −1.5 W/m^2 (C6-CMIP5, cyan). CAM6 ACI is reduced more than CAM5 ACI in response to CMIP5 emissions: CAM6 and C6-CMIP5 are farther than CAM5 and C5-CMIP5 in Figure 3d. Relative to CAM6 (black) with CMIP6 forcing, CAM5 (purple) has lower ACI in the subtropics but larger ACI in the Northern Hemisphere extratropics (Figure 3a). CAM6 includes ACI in the shallow cumulus regime in CAM6 with CLUBB. CAM6 also includes a reduction to the sensitivity of liquid autoconversion to cloud drop number (see the supporting information). The Seifert and Beheng (2001) representation of autoconversion (C6-SB, green dash) in CESM2d125 increases the magnitude of ACI from the modified Khairoutdinov and Kogan (2000) scheme in CAM6 but decreased it from the C6-KKorig simulation (Figure 3, red solid; Table S4). The C6-FixDN simulation (orange) was an experiment to remove dependence of autoconversion on cloud drop number. This removes any dependence of liquid water path (LWP) on aerosols (Figure 3d, orange) but does not result in different drop number sensitivity (Figure 3c). The total contribution from drop number changes alone (Twomey, 1977) in CAM6 (C6-FixDN) is ∼1.4 W/m^2. The 40% reduction in ACI (C6-FixDN vs. C6-SB) is consistent with estimates from Gettelman (2015).

Several other parameter changes (see the supporting information) have moderate impacts on ACI. Turbulent entertainment (C6-gam, light green) and SO_2 lifetime (C6-SO2, green solid) changes between CESM2d125 and CESM2 have little impact on ACI. Removing the (Hoose et al., 2010) mixed phase ice nucleation dependence on aerosols decreases ACI slightly (CAM6 vs. C6-IceNuc, red dotted), due to lower ΔLWP at higher latitudes with the original scheme in the C6-IceNuc experiment. The use of the original formulation of the Khairoutdinov and Kogan (2000) autoconversion scheme (C6-KK2000orig, red solid) produces the strongest ACI.

4. Discussion: Evolution of CESM2 From CESM2d125

The CESM2 development process evolved through many (299) different coupled model configurations. The critical criteria used to evaluate coupled experiments was whether they produced a PI (1850) control simulation in equilibrium (top of atmosphere net radiative fluxes <0.1 W/m^2) and whether the model reproduced gross features of the observed global annual mean surface temperature record, which include a period of warming from 1920–1940 and sustained warming from 1960 onward (see Figure S2). The twentieth century surface temperature record was used to guide model development but was not used to explicitly tune the model. Reasonable simulations by these metrics were achieved with the CESM2d125 configuration, which contained almost all of the final parameterizations for each component, using aerosol emissions from CMIP5 (Lamarque et al., 2010; Taylor et al., 2012). This configuration has an ECS of 4.4 K (Table 1). Increased ECS between CESM1 and CESM2d125 was a combination of higher CFs damped by a strong land model evaporation response to surface temperature and CO_2 increases (section 3.1).

From CESM2d125, CMIP6 emissions (Hoesly et al., 2018) were applied, resulting in simulations that did not match the observed twentieth century surface temperature record. A series of investigations indicated that CMIP6 emissions caused an increase in the magnitude of (negative) radiative forcing from aerosols and significant increases in the SW ACI (Figure 3). CAM6 is more sensitive than CAM5 to CMIP6 emissions.

The CESM2 development process assumed that the aerosol forcing is not well constrained and contains significant uncertainty. CESM2 ACI includes a large LWP response to aerosols (Figure 3b), which is difficult to support with observations (e.g., Malavelle et al., 2017), although recent work by Rosenfeld et al. (2019) provides some observational support for large LWP response and large magnitude ACI. A series of approaches were investigated to reduce ACI (Figure 3). As changes were made targeting improved ACI, this also necessitated changes to other uncertain parameters in the simulations ("model tuning"; Hourdin et al., 2016). Many of these parameters were related to clouds. Several of the changes made for purposes of adjusting ACI (e.g., the change to autoconversion from C6-SB in CESM2d125 to the final adjusted KK2000 version, SO2 and Gamma changes) seen in Figure 3 also impact CFs (Figure 1). CFs and ECS were not specifically adjusted or assessed the process, but parameters and parameterizations that were changed for other reasons also affected CFs and hence ECS.

5. Conclusions

The CESM2 ECS is 5.3 K, diagnosed with SOM simulations, an increase of over 1 K from CESM1. Higher ECS in CESM2 compared to CESM1 appears to be a consequence of changes to CFs and altering ACI to match the twentieth century temperature record, which also impacted feedbacks. CESM2 ECS is similar to the Energy Exascale Earth System Model version 1 (E3SMv1; Golaz et al., 2019). EASMv1 branched off from an atmosphere model similar to CAM6d125, though with a different development trajectory thereafter.

The land model parameter set used in the intermediate CESM2d125 version (CLM5d125) appears to have damped ECS, likely masking larger CFs from CAM6 physical parameterizations. Land model changes from CLM4 (CESM1) to CLM5 (CESM2) do not seem to be a significant contributor to the higher climate sensitivity in CESM2, though further investigation is required to definitely demonstrate this. The atmosphere model in CESM2d125, CAM6d125, has higher CFs than CAM5, due to changes in (1) stratiform cloud microphysics, (2) unified turbulence, (3) ice nucleation, and (4) convective changes increasing LWCFs.

The final process of developing CESM2 was strongly affected by altering the ACI to adjust to a new emissions data set, which increased the magnitude of ACI in CESM2. Many of the changes to reduce ACI between CESM2d125 and CESM2 also have affected CFs and ECS, especially rain formation (SB2001) and evaporation (MG2precip) processes and the SO_2 lifetime. ECS and feedbacks were never explicitly tuned in CESM2, but the ACI was explicitly adjusted downward.

This work demonstrates the complex coupling between climate forcing and climate feedbacks, particularly through the nexus of clouds (Gettelman et al., 2016). In complex ESMs such as CESM2, forcing and feedback are not independent variables, and indeed, they covary (Kiehl, 2007): Processes affecting one will affect the other. The interaction of spatially varying forcing and feedbacks is a subject for future work.

CFs are the cause of increased ECS in CESM2. But the cloud distribution in CESM2 is significantly improved over CESM1 in many ways. CESM2 compares well to observations, better than CESM1 (see the supporting

information), which was already one of the "better" models in CMIP5 (Knutti et al., 2013). An ECS of 5.3 K would lead to a high level of climate change and large impacts. It is imperative that the community work in a multimodel context to understand how plausible such a high ECS is. What scares us is not that the CESM2 ECS is wrong (all models are wrong, [Box, 1976]) but that it might be right.

Acknowledgments
The CESM project is supported primarily by the National Science Foundation (NSF). This material is based upon work supported by the National Center for Atmospheric Research, which is a major facility sponsored by the NSF under Cooperative Agreement 1852977. Portions of this study were supported by the Regional and Global Model Analysis (RGMA) component of the Earth and Environmental System Modeling Program of the U.S. Department of Energy's Office of Biological and Environmental Research (BER) Cooperative Agreement DE-FC02-97ER62402. Computing and data storage resources, including the Cheyenne supercomputer (doi:10.5065/D6RX99HX), were provided by the Computational and Information Systems Laboratory (CISL) at NCAR. CESM1 and CESM2 code bases are available via links from http://www.cesm.ucar.edu/models/. Summary data for the simulations provided in this manuscript is available at ftp://ftp.cgd.ucar.edu/archive/andrew/cesm2ecs. Raw model output from simulations in this paper is available at: https://doi.org/10.26024/zrad-5z41.

References

Ackerman, A. S., Kirkpatrick, M. P., Stevens, D. E., & Toon, O. B. (2004). The impact of humidity above stratiform clouds on indirect aerosol climate forcing. *Nature*, *432*, 1014–1017.

Albrecht, B. A. (1989). Aerosols, cloud microphysics and fractional cloudiness. *Science*, *245*, 1227–1230.

Bogenschutz, P. A., Gettelman, A., Morrison, H., Larson, V. E., Craig, C., & Schanen, D. P. (2013). Higher-order turbulence closure and its impact on Climate Simulation in the Community Atmosphere Model. *Journal of Climate*, *26*(23), 9655–9676. https://doi.org/10.1175/JCLI-D-13-00075.1

Bony, S., Colman, R., Kattsov, V. M., Allan, R. P., Bretherton, C. S., Dufresne, J.-L., et al. (2006). How well do we understand and evaluate climate change feedback processes? *Journal of Climate*, *19*(15), 3445–3482. https://doi.org/10.1175/JCLI3819.1

Boucher, O., Randall, D., Artaxo, P., Bretherton, C., Feingold, G., Forster, P., et al. (2013). Clouds and Aerosols. In T. F. Stocker, D. Qin, G.-K. Plattner, M. Tignor, S. K. Allen, J. Boschung, et al. (Eds.), *Climate change 2013: The physical science basis. Contribution of Working Group I to the Fifth Assessment Report of the Intergovernmental Panel on Climate Change* (pp. 571–657). Cambridge, UK: Cambridge Universtiy Press.

Box, G. E. P. (1976). Science and statistics. *Journal of the American Statistical Association*, *71*(356), 791–799. https://doi.org/10.1080/01621459.1976.10480949

Cess, R. D. (2005). Water vapor feedback in climate models. *Science*, *310*, 795–796.

Cess, R. D., Potter, G. L., Blanchet, J. P., Boer, G. J., Del Genio, A. D., Déqué, M., et al. (1990). Intercomparison and interpretation of climate feedback processes in 19 atmospheric general circulation models. *Journal Geophysical Research*, *95*, 16,601–16,615.

Cess, R. D., Potter, G. L., Blanchet, J. P., Boer, G. J., Ghan, S. J., Jeffrey, T., et al. (1989). Interpretation of cloud-climate feedback as produced by 14 atmospheric general circulation models. *Science*, *245*, 513–516.

Charney, J. G. (1979). Carbon dioxide and climate: A scientific assessment (Tech. Rep.) Washington, DC: National Academy of Science.

Collins, W. D., Ramaswamy, V., Schwarzkopf, M. D., Sun, Y., Portmann, R. W., Fu, Q., et al. (2006). Radiative forcing by well-mixed greenhouse gases: Estimates from climate models in the Intergovernmental Panel on Climate Change (IPCC) Fourth Assessment Report (AR4). *Journal of Geophysical Research*, *111*, D14317. https://doi.org/10.1029/2005JD006713

Colman, R. A. (2013). Surface albedo feedbacks from climate variability and change. *Journal of Geophysical Research: Atmospheres*, *118*, 2827–2834. https://doi.org/10.1002/jgrd.50230

Danabasoglu, G., & Gent, P. R. (2009). Equilibrium climate sensitivity: Is it accurate to use a slab ocean model? *Journal of Climate*, *22*(9), 2494–2499. https://doi.org/10.1175/2008JCLI2596.1

Eyring, V., Bony, S., Meehl, G. A., Senior, C. A., Stevens, B., Stouffer, R. J., & Taylor, K. E. (2016). Overview of the Coupled Model Intercomparison Project Phase 6 (CMIP6) experimental design and organization. *Geoscientific Model Development*, *9*(5), 1937–1958. https://doi.org/10.5194/gmd-9-1937-2016

Folkins, I. (2002). Origin of lapse rate changes in the upper tropical troposphere. *Journal of Atmospheric Sciences*, *59*, 992–1005.

Gettelman, A. (2015). Putting the clouds back in aerosol–cloud interactions. *Atmospheric Chemistry and Physics*, *15*(21), 12,397–12,411. https://doi.org/10.5194/acp-15-12397-2015

Gettelman, A., Fasullo, J. T., & Kay, J. E. (2013). Spatial decomposition of climate feedbacks in the Community Earth System Model. *Journal Climate*, *40*, 3544–2561. https://doi.org/10.1175/JCLI-D-12-00497.1

Gettelman, A., Kay, J. E., & Shell, K. M. (2012). The evolution of climate feedbacks in the Community Atmosphere Model. *Journal of Climate*, *25*(5), 1453–1469. https://doi.org/10.1175/JCLI-D-11-00197.1

Gettelman, A., Lin, L., Medeiros, B., & Olson, J. (2016). Climate feedback variance and the interaction of aerosol forcing and feedbacks. *Journal of Climate*, *29*(18), 6659–6675. https://doi.org/10.1175/JCLI-D-16-0151.1

Gettelman, A., Liu, X., Barahona, D., Lohmann, U., & Chen, C. C. (2012). Climate impacts of ice nucleation. *Journal of Geophysical Research*, *117*, D20201. https://doi.org/10.1029/2012JD017950

Gettelman, A., & Morrison, H. (2015). Advanced two-moment bulk microphysics for global models. Part I: Off-line tests and comparison with other schemes. *Journal of Climate*, *28*(3), 1268–1287. https://doi.org/10.1175/JCLI-D-14-00102.1

Gettelman, A., Morrison, H., Santos, S., Bogenschutz, P., & Caldwell, P. M. (2015). Advanced two-moment bulk microphysics for global models. Part II: Global model solutions and aerosol-cloud interactions. *Journal of Climate*, *28*(3), 1288–1307. https://doi.org/10.1175/JCLI-D-14-00103.1

Gettelman, A., & Sherwood, S. C. (2016). Processes responsible for cloud feedback. *Current Climate Change Reports*, *2*, 179–189. https://doi.org/10.1007/s40641-016-0052-8

Golaz, J.-C., Caldwell, P. M., Van Roekel, L. P., Petersen, M. R., Tang, Q., Wolfe, J. D., et al. (2019). The DOE E3SM coupled model version 1: Overview and evaluation at standard resolution. *Journal of Advances in Modeling Earth Systems*, *11*. https://doi.org/10.1029/2018MS001603

Hansen, J., Sato, M. K. I., Ruedy, R., Nazarenko, L., Lacis, A., Schmidt, G. A., et al. (2005). Efficacy of climate forcings. *Journal of Geophysical Research*, *110*, D18104. https://doi.org/10.1029/2005JD005776

Held, I. M., & Soden, B. J. (2000). Water vapor feedback and global warming. *Annual Review of Environment and Resources*, *25*, 441–75.

Hoesly, R. M., Smith, S. J., Feng, L., Klimont, Z., Janssens-Maenhout, G., Pitkanen, T., et al. (2018). Historical (1750–2014) anthropogenic emissions of reactive gases and aerosols from the Community Emissions Data System (CEDS). *Geoscientific Model Development*, *11*(1), 369–408. https://doi.org/10.5194/gmd-11-369-2018

Hoose, C., Kristjánsson, J. E., Chen, J.-P., & Hazra, A. (2010). A classical-theory-based parameterization of heterogeneous ice nucleation by mineral dust, soot, and biological particles in a global climate model. *Journal of the Atmospheric Sciences*, *67*(8), 2483–2503. https://doi.org/10.1175/2010JAS3425.1

Hourdin, F., Mauritsen, T., Gettelman, A., Golaz, J.-C., Balaji, V., Duan, Q., et al. (2016). The art and science of climate model tuning. *Bulletin of the American Meteorological Society*, *98*, 589–602. https://doi.org/10.1175/BAMS-D-15-00135.1

Hurrell, J. W., Holland, M., Gent, P., Ghan, S., Kay, J. E., Kushner, P., et al. (2013). The Community Earth System Model: A framework for collaborative research. *Bulletin of the American Meteorological Society*, *94*(9), 1339–1360. https://doi.org/10.1175/BAMS-D-12-00121.1

Kay, J. E., Deser, C., Phillips, A., Mai, A., Hannay, C., Strand, G., et al. (2014). The Community Earth System Model (CESM) large ensemble project: A community resource for studying climate change in the presence of internal climate variability. *Bulletin of the American Meteorological Society*, *96*, 1333–1349. https://doi.org/10.1175/BAMS-D-13-00255.1

Khairoutdinov, M. F., & Kogan, Y. (2000). A new cloud physics parameterization in a large-eddy simulation model of marine stratocumulus. *Monthly Weather Review*, *128*, 229–243.

Kiehl, J. T. (2007). Twentieth century climate model response and climate sensitivity. *Geophysical Research Letters*, *34*, L22710. https://doi.org/10.1029/2007GL031383

Knutti, R., Masson, D., & Gettelman, A. (2013). Climate model genealogy: Generation CMIP5 and how we got there. *Geophysical Research Letters*, *40*, 1194–1199. https://doi.org/10.1002/grl.50256

Knutti, R., Rugenstein, M. A. A., & Hegerl, G. C. (2017). Beyond equilibrium climate sensitivity. *Nature Geosci*, *10*, 727–736. https://doi.org/10.1038/ngeo3017

Lamarque, J.-F., Bond, T. C., Eyring, V., Granier, C., Heil, A., Klimont, Z., et al. (2010). Historical (1850–2000) gridded anthropogenic and biomass burning emissions of reactive gases and aerosols: Methodology and application. *Atmospheric Chemistry and Physics*, *10*(15), 7017–7039. https://doi.org/10.5194/acp-10-7017-2010

Malavelle, F. F., Haywood, J. M., Jones, A., Gettelman, A., Clarisse, L., Bauduin, S., et al. (2017). Strong constraints on aerosol-cloud interactions from volcanic eruptions. *Nature*, *546*(7659), 485–491. https://doi.org/10.1038/nature22974

Meyers, M. P., DeMott, P. J., & Cotton, W. R. (1992). New primary ice-nucleation parameterizations in an explicit cloud model. *Journal of Applied Meteorology*, *31*, 708–721.

Park, S., & Bretherton, C. S. (2009). The University of Washington shallow convection and moist turbulence schemes and their impact on climate simulations with the Community Atmosphere Model. *Journal of Climate*, *22*, 3449–3469.

Pendergrass, A. G., Conley, A., & Vitt, F. M. (2018). Surface and top-of-atmosphere radiative feedback kernels for CESM-CAM5. *Earth System Science Data*, *10*(1), 317–324. https://doi.org/10.5194/essd-10-317-2018

Rosenfeld, D., Zhu, M., Wang, Y., Zheng, T., Goren, T., & Yu, S. (2019). Aerosol-driven droplet concentrations dominate coverage and water of oceanic low-level clouds. *Science*, *363*(6427), eaav0566. https://doi.org/10.1126/science.aav0566

Seifert, A., & Beheng, K. D. (2001). A double-moment parameterization for simulating autoconversion, accretion and selfcollection. *Atmospheric Research*, *59–60*, 265–281.

Shell, K. M., Kiehl, J. T., & Shields, C. A. (2008). Using the radiative kernel technique to calculate climate feedbacks in NCAR's Community Atmosphere Model. *Journal of Climate*, *21*, 2269–2282. https://doi.org/10.1175/2007JCLI2044.1

Sherwood, S. C., Bony, S., Boucher, O., Bretherton, C., Forster, P. M., Gregory, J. M., & Stevens, B. (2015). Adjustments in the forcing-feedback framework for understanding climate change. *Bulletin of the American Meteorological Society*, *96*(2), 217–228. https://doi.org/10.1175/BAMS-D-13-00167.1

Soden, B. J., Held, I. M., Colman, R., Shell, K. M., Kiehl, J. T., & Shields, C. A. (2008). Quantifying climate feedbacks using radiative kernels. *Journal of Climate*, *21*(14), 3504–3520. https://doi.org/10.1175/2007JCLI2110.1

Stephens, G. L. (2005). Cloud feedbacks in the climate system: A critical review. *Journal of Climate*, *18*(2), 237–273.

Stevens, B., & Feingold, G. (2009). Untangling aerosol effects on clouds and precipitation in a buffered system. *Nature*, *461*(1), 607–613.

Stocker, T. F., Qin, D., Plattner, G. K., Tignor, M., Allen, S. K., Boschung, J., et al. (2013). IPCC, 2013: Climate change 2013: The physical science basis. Contribution of working group I to the fifth assessment report of the intergovernmental panel on climate change.

Taylor, K. E., Stouffer, R. J., & Meehl, G. A. (2012). An overview of CMIP5 and the experimental design. *Bulletin of the American Meteorological Society*, *93*, 485–498. https://doi.org/10.1175/BAMS-D-11-00094.1

Tian, B. (2015). Spread of model climate sensitivity linked to double-Intertropical Convergence Zone bias. *Geophysical Research Letters*, *42*, 4133–4141. https://doi.org/10.1002/2015GL064119

Twomey, S. (1977). The influence of pollution on the shortwave albedo of clouds. *Journal of the Atmospheric Sciences*, *34*(7), 1149–1152.

Vial, J., Bony, S., Stevens, B., & Vogel, R. (2017). Mechanisms and model diversity of trade-wind shallow cumulus cloud feedbacks: A review. *Surveys in Geophysics*, *38*(6), 1331–1353. https://doi.org/10.1007/s10712-017-9418-2

Webb, M. J., Lambert, F. H., & Gregory, J. M. (2012). Origins of differences in climate sensitivity, forcing and feedback in climate models. *Climate Dynamics*, *40*, 677–707.

Zelinka, M. D., Zhou, C., & Klein, S. A. (2016). Insights from a refined decomposition of cloud feedbacks. *Geophysical Research Letters*, *43*, 9259–9269. https://doi.org/10.1002/2016GL069917